Trivalent iron-tartaric acid metal-organic framework for catalytic ozonation of succinonitrile

Song Wang, Genwang Zhu, Zhongchen Yu, Chenxi Li, Dan Wang and Xiaoling Cao

ABSTRACT

As porous crystal materials, metal-organic frameworks (MOFs) have attracted wide attention in the field of environmental remediation. In this study, a trivalent iron-tartaric acid metal-organic framework (T2-MOF) was successfully synthesized using the inexpensive raw materials ferric chloride ($FeCl_3.6H_2O$) and tartaric acid ($C_4H_6O_6$). The physical and chemical properties of T2-MOF were studied by using X-ray diffraction, Fourier transform infrared spectroscopy, scanning electron microscopy, energy-dispersive X-ray spectroscopy, X-ray photoelectron spectroscopy and Brunauer–Emmett–Teller. After that, T2-MOF was used as a catalyst for catalytic ozonation of succinonitrile. The results show that T2-MOF has obvious crystal characteristics and uniform structure. In addition, T2-MOF exhibits strong catalytic performance in ozonation of succinonitrile. The results indicate that the chemical oxygen demand (COD) removal rate is affected by various operating parameters including catalyst characteristics dosages and initial pH values. In the ozonation with 30 mg L^{-1} T2-MOF, the COD removal rate of 100 mg L^{-1} succinonitrile reached 73.1% ($\pm$4.6%) within 180 min, which was 67.3% ($\pm$4.4%) higher than that obtained in the process without catalyst. T2-MOF maintained strong catalytic performance with the pH range of 3.0–7.0. By monitoring the Fe^{2+} concentration at different reaction time, it was found that the homogeneous catalysis occurred simultaneously with the heterogeneous catalysis.

Key words | catalytic mechanism, catalytic ozonation, metal-organic framework, orthogonal experiments, succinonitrile, wastewater treatment

Song Wang
Genwang Zhu
Dan Wang
School of Earth Science,
Northeast Petroleum University,
Daqing 163318,
China

Zhongchen Yu (corresponding author)
Xiaoling Cao
School of Civil Architecture Engineering,
Northeast Petroleum University,
Daqing 163318,
China
E-mail: yuzi7777@163.com

Chenxi Li
School of Engineering,
Heilongjiang Bayi Agricultural University,
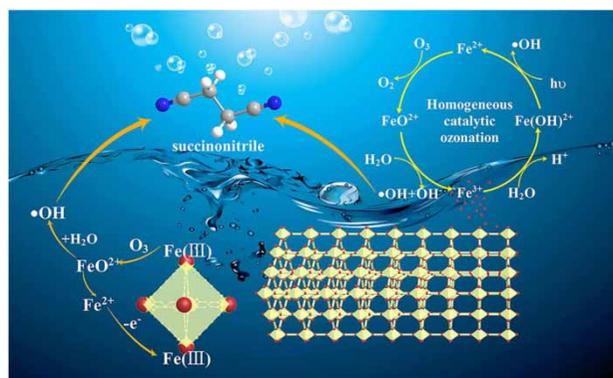Daqing,
China

HIGHLIGHTS

- A metal-organic framework was synthesized using trivalent iron and tartaric acid.
- This metal-organic framework, named T2-MOF, exhibited high activity for the catalytic ozonation of succinonitrile.
- Orthogonal experiments established the priority of different influencing factors.
- The dissociative Fe^{2+} and Fe^{3+} demonstrated that homogeneous and heterogeneous reactions occurred in the same system.
- After five cycles of experimental use, T2-MOF showed strong reusability.

GRAPHICAL ABSTRACT

INTRODUCTION

Acrylic fiber wastewater is recognized as a serious organic pollutant due to its high toxicity and persistence in the environment (Sun *et al.* 2015; Hu *et al.* 2016). Succinonitrile is the main refractory organic component of acrylic fiber wastewater. Therefore, the development of an effective wastewater treatment technology for succinonitrile would be very beneficial to the treatment of acrylic fiber wastewater.

In the last few decades, advanced oxidation processes (AOPs) have been regarded as effective techniques for treating wastewater containing refractory organic pollutants (Chong *et al.* 2010). In earlier reports, different oxidants in AOPs, such as hydrogen peroxide (H_2O_2), persulfate and ozone (O_3), have been compared (Lian *et al.* 2017). H_2O_2 requires careful control of pH (2.5–4.0). Cl^- inhibits the destruction of organic contaminants by persulfate-based AOPs (Huang *et al.* 2016). The above disadvantages make the use of H_2O_2 and persulfate difficult in industrialized applications. AOPs based on ozone have many attractive advantages, including low cost and lower residuals after treatment, which mean that AOPs based on ozone have broad application prospects.

At present, a more in-depth and feasible method is catalytic ozone oxidation (Mohapatra & Kirpalani 2019). There are usually two forms of catalytic ozone oxidation, homogeneous catalytic ozonation and heterogeneous catalytic ozonation. Homogeneous catalytic ozonation is fast and efficient, but it has the disadvantages of harsh reaction conditions, large catalyst dosage and secondary pollution. Heterogeneous catalytic ozonation has attracted the attention of many researchers due to the advantages of easy catalyst recovery and mild reaction conditions. In recent years, researchers have continuously developed new heterogeneous catalysts to improve the efficiency of ozone catalysis (Gayen *et al.* 2018).

The large number of catalytic sites in the heterogeneous catalyst can effectively improve the catalytic efficiency. Previous studies have shown that the greater the specific surface area of the heterogeneous catalyst, the more catalytic sites it contains (Gassie & Englehardt 2017). Therefore, increasing the specific surface area of the catalyst is an attractive development direction for heterogeneous catalytic ozonation.

In 1995, Yaghi *et al.* (1995) first reported a two-dimensional coordination compound synthesized from 1,3,5-benzenetricarboxylate (BTC) and cobaltous nitrate. The compound was named a metal-organic framework (MOF). Such materials are composed of transition metal ions containing vacant orbitals and organic bridge bonds formed through self-assembly (Zhou *et al.* 2012). MOFs exhibit diverse physical and chemical properties, such as a high surface area, controllable pore volume and thermal stability, etc. (Easun *et al.* 2017). Due to these unique properties, researchers have tried to synthesize various new MOFs for different fields (Hidalgo *et al.* 2018; Li *et al.* 2018). Tang & Wang (2018) used a CUS-MIL-100(Fe) catalytic H_2O_2 system to decompose sulfamethazine (SMT), and the degradation efficiency of SMT reached 100% after 100 min. Araya *et al.* (2017) used MIL-53(Fe) to photodegrade sulforhodamine B (SRB), and the removal rate of SRB was 96% after 120 min.

Although MOFs have enabled remarkable progress in the field of environmental remediation, there are also some disadvantages. Some reports about the application of

MOFs in environmental remediation are shown in Table S1 in the Supplementary Information. MOFs exhibit diverse physical and chemical properties, such as a high surface area, controllable pore volume, thermal stability, etc. Due to these unique properties, MOFs have attracted extensive attention from researchers in wastewater treatment. However, the cost of the organic ligands (1,4-dicarboxybenzene, 1,3,5-benzenetricarboxylic acid, 2-methylimidazole etc.) used to synthesize these MOFs is high, which limits the application of these MOFs.

Most of the reported AOPs reactions have been carried out in the liquid phase. Moisture will destroy the structure of MOFs, causing them to irreversibly collapse, thereby reducing their specific surface area and pore volume. This structural collapse can reduce the catalytic performance of MOFs in AOPs (Guo *et al.* 2015). Thus, in order to improve the structural strength of MOFs, different researchers have proposed different solutions. Kim *et al.* (2001) noted that the large reticular crystal structure of MOFs was formed by the directional growth of metal-oxygen-carbon clusters with very stable chemical bonds, and these special clusters were defined as secondary building units (SBUs). Yaghi *et al.* (2003) suggested that a large number of hydroxyl or carboxyl groups could strengthen SBUs to increase the structural strength of MOFs. Each tartaric acid has two hydroxyl groups and two carboxyl groups, and is an ideal raw for the synthesis of MOFs. Moreover, it is widely present in higher plants and is low in cost.

In this work, a solvothermal method was employed to synthesize tartaric acid MOF (T2-MOF) precursors by the reaction of ferric chloride and tartaric acid with more carboxyl groups in a mixed solvent of N,N-dimethylformamide (DMF) at 105 °C for 24 hours. The factors affecting the degradation of succinonitrile by T2-MOF catalyzed ozone and reaction kinetics were studied.

MATERIALS AND METHODS

Materials

Ferric chloride, N,N-dimethylacetamide (DMA), sodium sulfate, sodium chloride, sodium hydroxide and tartaric acid were purchased from DAMAO (Tianjin, China). Mercury sulfate, silver sulfate, sulfuric acid, sodium carbonate and potassium dichromate were purchased from Kermel Chemical Reagents Company (Tianjin, China). All reagents were analytical grade. Succinonitrile (>99%) was purchased from J&K Scientific (Beijing, China).

Preparation of T2-MOF

In a typical procedure, 3.0 mmol $FeCl_3.6H_2O$ and 2.5 mmol $C_4H_6O_6$ were added slowly to 80 mL of DMA solution to prepared T2-MOF by a mild solvothermal reaction. The mixture was stirred at room temperature for 10 min, and then transferred into a Teflon-lined stainless-steel autoclave with a volume capacity of 150 mL. The autoclave was heated at 105 °C for 24 hours then allowed to cool naturally to room temperature. The prepared catalysts were filtered through common commercial qualitative filter paper. The pore size of the filter paper was 30–50 μm, and the material was cotton fiber. A yellow powder was obtained at the bottom of the autoclave. The yellow powder was filtered and washed four times, alternately using distilled water and acetone, followed by natural air drying 3 hours to obtain T2-MOF (Figure S1).

Characterization of T2-MOF

X-ray diffraction (XRD) with monochromatized Cu $K\alpha$ radiation ($\lambda = 0.15418$ nm) was used to analyze the crystallinity of the as-synthesized T2-MOF (Model: Rigaku D/max-2200PC). Fourier transform infrared spectroscopic (FT-IR) was employed to investigate the chemical structure and identify the functional groups of the prepared T2-MOF (Model: IRTracer-100 FT-IR Spectrometric Analyzer). Scanning electron microscope (SEM) analysis was performed to observe the morphology of the T2-MOF (Model: Quanta 200). Energy-dispersive X-ray spectroscopy (EDS) equipped with an SEM was used to analyze the elemental composition of the T2-MOF. Surface electronic states of T2-MOF were analyzed with X-ray photoelectron spectroscopy (XPS) (Model: ESCALAB250Xi). The Brunauer–Emmett–Teller (BET) surface area and porous structure of T2-MOF were measured by N_2 adsorption–desorption isotherms at 77 K (Model: ASAP 2020 PLUS HD88).

Degradation experiments

The ozonation of succinonitrile using T2-MOF as a catalyst was tested in a cylindrical organic glass reactor with a working volume of 5 L. A total of 150 mg T2-MOF was added. Ozone gas with a flux ranging from 20 mg L^{-1} to 25 mg L^{-1} was generated from a GUOLIN generator. The hydraulic retention time (HRT) was 180 min. At predetermined time intervals, the suspension was extracted and then centrifuged to obtain the supernatant for analysis.

The degradation effect of succinonitrile was indicated by COD. In the process, the trivalent iron on the surface of the T2-MOF can dissolve into solution. The dissolved trivalent ions can cause a homogeneous catalytic reaction and produce Fe^{2+}. Therefore, the concentrations of Fe^{2+} and Fe^{3+} were determined by o-phenanthroline spectrophotometry at 510 nm (Model: 752N). The pH of the succinonitrile solution was adjusted by adding 0.1 mol L^{-1} H_2SO_4 and 0.1 mol L^{-1} NaOH and was determined by a pH meter (Model: PHS-3C).

Inorganic anion scavenging experiment

There are various reactive oxygen species (ROS) that play important roles in AOPs. As we know, many inorganic anions exist in wastewater, such as CO_3^{2-}, Cl^- and SO_4^{2-}, and they may pose a threat to attaining the right catalytic property. The roles of sodium sulfate (Na_2SO_4) sodium chloride (NaCl) and sodium carbonate (Na_2CO_3) in the catalytic ozonation of succinonitrile system were studied because these inorganic anions may be scavengers for various ROS. Before every experiment, only one inorganic salt (10 mmol L^{-1}) was added to the experimental system under initial reaction conditions.

Analysis of orthogonal experiments

Orthogonal experiments are a method for scientifically arranging and analyzing multifactor experiments using orthogonal tables. It is one of the most commonly used experimental design methods. The degradation of succinonitrile was mainly influenced by the initial pH, HRT and dosage of T2-MOF. To obtain the optimal reaction conditions and the order of importance of each factor, an orthogonal experiment was designed. Each factor had five levels, and the levels of the experimental factors are shown in Table S2. The orthogonal experimental design was $L_{25}5^6$, as shown in Table S3. A detailed discussion of this section can be found in the Supplementary Information.

RESULTS AND DISCUSSION

Characterization of the T2-MOF

XRD was used to characterize the crystallographic structure of the T2-MOF and $FeCl_3.6H_2O$. As presented in Figure 1(a), the different diffraction peaks from T2-MOF and $FeCl_3.6H_2O$ indicate that the crystal structure of T2-MOF was different from that of $FeCl_3.6H_2O$. Moreover, the strong diffraction peaks at 15.18°, 19.84° and 25.1° corresponding to the (200), (−111) and (020) reflections indicate that the T2-MOF had three preferred orientations (Zeng *et al.* 2015). These changes in crystal structure suggested that T2-MOF was synthesized.

The prepared T2-MOF was analyzed by FT-IR spectroscopy, and the result is shown in Figure 1(b). The peaks from 700 to 1,300 cm^{-1} could be assigned to C–H bending vibrations (Hermes *et al.* 2006). The characteristic absorption peak observed at 1,419 cm^{-1} was derived from the vibration of C–O bonds in the carboxylate groups of tartaric acid. The characteristic absorption peak at 3,422 cm^{-1} was attributed to polyhydroxyl groups in tartaric acid. Therefore, the combined results of XRD analysis and FT-IR spectroscopy clearly confirmed the formation of T2-MOF.

The morphology of T2-MOF sample was observed by SEM. As shown in Figure 2(a) and 2(b), many rod-like
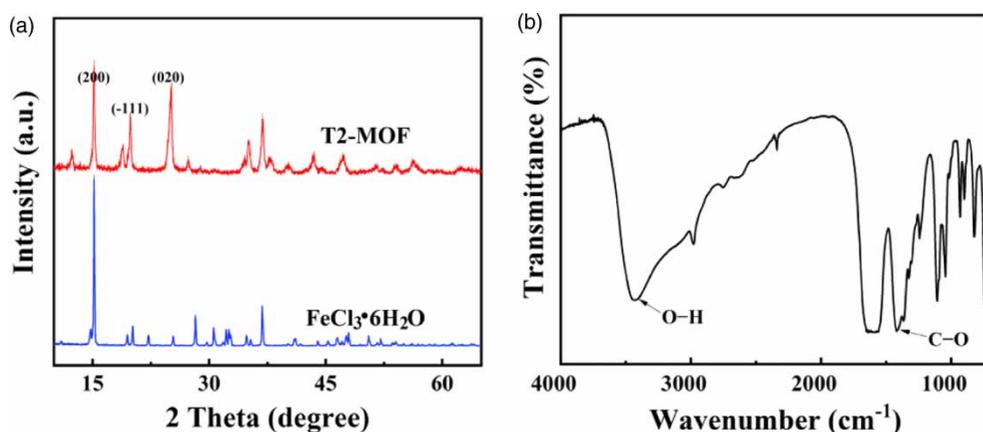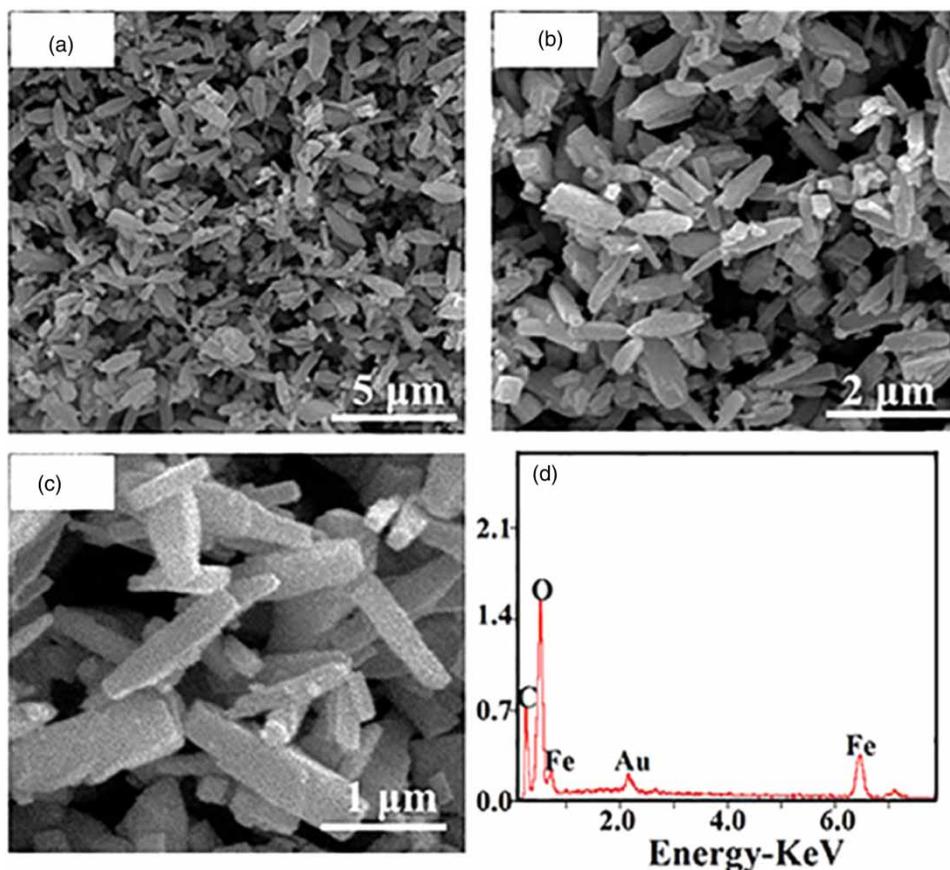

Figure 1 | (a) XRD patterns of T2-MOF and $FeCl_3.6H_2O$. (b) FT-IR spectrum of T2-MOF.

Figure 2 | SEM images ((a), (b) and (c)) and EDS spectrum (d) of T2-MOF.

crystals are uniformly dispersed in the field of view. Further observation revealed that the crystal form of T2-MOF is distinct cubic structure (Figure 2(c)). The compositional analysis carried out by EDS measurements (Figure 2(d)) shows the presence of Fe, C and O elements in the T2-MOF sample. In addition, the EDS elemental mapping (Figure S2) further confirmed that these elements were evenly distributed in T2-MOF.

The detailed chemical components and electronic states of the T2-MOF were determined by XPS. The XPS survey spectrum and high-resolution XPS spectra of the T2-MOF are shown in Figure S3 and Figure 3, respectively. The
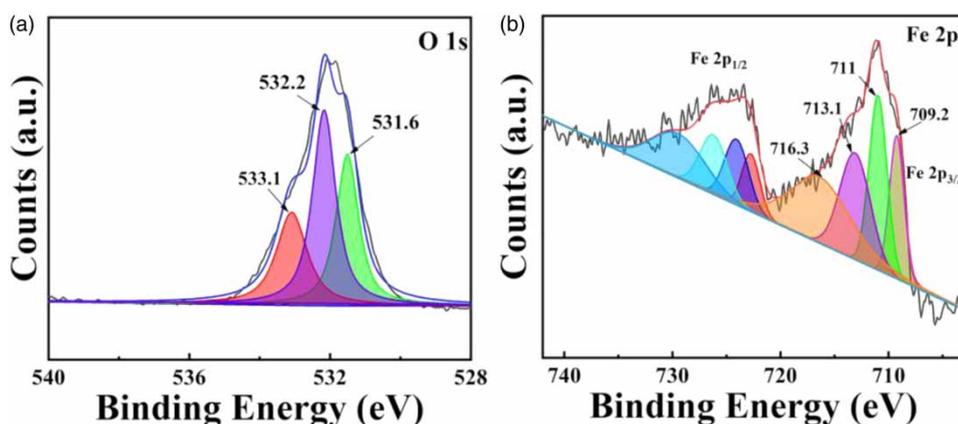
Figure 3 | XPS spectra of T2-MOF: (a) O 1s, and (b) Fe 2p.

XPS survey spectrum (Figure S3a) demonstrated that C, O, and Fe existed in the T2-MOF. The high-resolution XPS spectrum of C 1s (Figure S3b) could be fitted by two peaks at 284.9 eV and 288.7 eV, which were derived from single-bond carbon in tartaric acid and carboxylate groups, respectively (Ahimou *et al.* 2007). The peak at 288.7 eV was attributed to the double bond of carboxylate groups (Zhang *et al.* 2015). In the high-resolution XPS spectrum of O 1s (Figure 3(a)), each O 1s XPS peak is wide, showing that there was more than one electronic state. The binding energies of 531.6 eV and 532.2 eV are related to the hydroxyl groups of tartaric acid and single bonds between oxygen and carbon (C-O), respectively (Yu *et al.* 2019). The higher binding energy at 533.1 eV was attributed to the carboxyl groups of tartaric acid (Baldanza *et al.* 2016). Figure 3(b) shows the high-resolution XPS spectra of Fe 2p. The peaks at 711 eV and 713.1 eV are characteristic of Fe^{3+} in T2-MOF (Chandra *et al.* 2010). Overall, the XPS high-resolution spectra confirmed that the T2-MOF contained the expected components.

Specific surface area and porous structure of T2-MOF were measured by N_2 adsorption–desorption isotherms at 77 K. Figure 4(a) is the N_2 adsorption–desorption isotherms of T2-MOF displayed an intermediate mode between type I and type IV (Peng *et al.* 2012). The BET surface area and total pore volume of T2-MOF were calculated to be 24.9 $m^2\,g^{-1}$ and 0.070 $cm^3\,g^{-1}$, respectively. Calculated from the desorption branch of the nitrogen isotherm with the Barrett–Joyner–Halenda (BJH) analysis, the pore diameter of the T2-MOF was determined to be 14.23 nm (Figure 4(b)), while the illustration in figure S4 had shown the micropore size about 1.10 nm from the Horvath–Kawazoe method.

Catalytic activity of the T2-MOF

The COD removal rate was used to evaluate the degradation of succinonitrile in three ozonation systems: an ozone-alone system (OAS), trivalent iron-tartaric acid complex catalytic ozonation system (TCS) and T2-MOF catalytic ozonation system (MCS). The initial concentration of succinonitrile in the three catalytic ozonation systems was 100 mg L^{-1}, and the gas phase ozone concentration was approximately 20–25 mg L^{-1}. The pH was neutral. Figure S5a shows the variation in COD of succinonitrile with oxidation time in the various oxidation systems. In OAS, the decrease in COD associated with succinonitrile was 10.2 mg L^{-1} after 180 min; in combination with Figure 5(a), the COD removal rate was only 5.83%. In the other two oxidation systems involving catalysts, the COD reduction was significantly improved. Especially in MCS, the decrease in COD reduction was 134.5 mg L^{-1} (Figure S5a), and the corresponding COD removal rate reached 73.1% (Figure 5(a)). Moreover, the COD removal rate increased by 20.7% compared with that in TCS. These results indicate that T2-MOF is the most appropriate catalyst for catalyzing ozone to degrade succinonitrile in this study.

A comparison of data can highlight the improvement in catalyst performance. Despite the many papers we consulted, there are few reports on the treatment of succinonitrile by AOPs. We only found a master's thesis on the use of complexing agents to catalyze the degradation of succinonitrile by ozone. Zhong (2017) studied the effect of two catalysts for catalyzing ozone to degrade succinonitrile. In his study, the COD removal rates of succinonitrile catalyzed by Fe^{2+} ions alone and Fe^{2+}/sodium pyrophosphate were 35.7% and 49.7%, respectively. Compared with the two
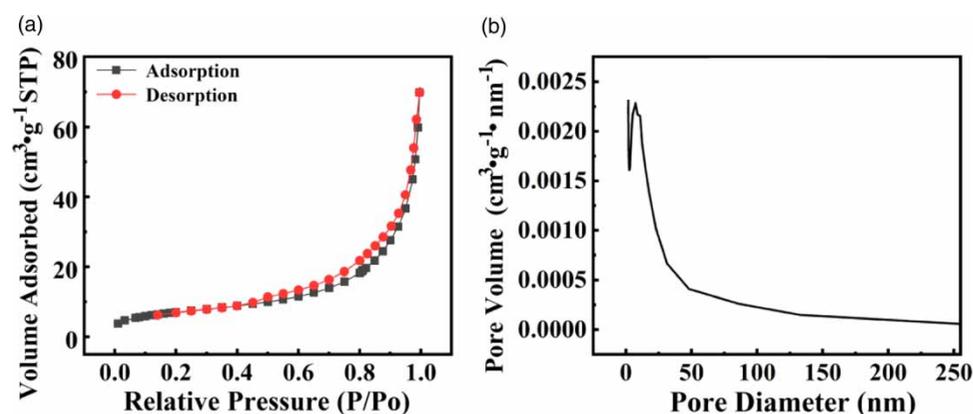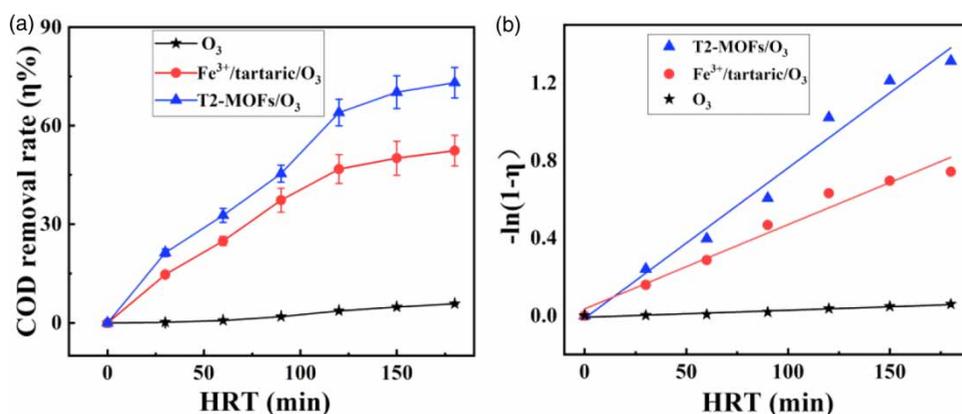

Figure 4 │ (a) Nitrogen adsorption–desorption isotherms of T2-MOF. (b) The Barrett–Joyner–Halenda (BJH) mesoporous size distribution of T2-MOF.

Figure 5 | (a) COD removal rate of succinonitrile in different systems. (b) Pseudo-first-order kinetics curves for the degradation of succinonitrile in different systems.

catalysts reported by Zhong, T2-MOF increases the catalytic efficiency by 105% and 47.1%, respectively. This comparison shows that the catalytic performance of T2-MOF is excellent.

As the main component of acrylic fiber wastewater, succinonitrile is more difficult to degrade than acrylic fiber wastewater. Therefore, to improve the reliability of the comparison results, we compared two catalysts used in the treatment process similar to our work. An *et al.* (2011) studied the ozonation of acrylic fiber wastewater by synergized ultraviolet light. The results showed that the COD removal rate was only 25% under optimal conditions. In addition, Wei *et al.* (2013) studied the treatment of acrylic fiber wastewater by a Fenton process under acidic conditions. The results indicated that the COD removal rate was only 47% after 2 hours. As the main component of acrylic fiber wastewater, succinonitrile is the focus and the most challenging aspect of acrylic fiber wastewater treatment. In comparison with the above research, T2-MOF increased the catalytic efficiency by 2.9 and 1.6 times, respectively. This comparison shows that the performance of T2-MOF catalyzed ozone to degrade succinonitrile is excellent.

Benitez *et al.* (1999) demonstrated that the decomposition of organic compounds by ozone proceeds via a pseudo-first-order reaction. That is, in the process of organic pollutant decomposition by ozone, the degradation rate of organic matter satisfies the following:

$$-\frac{\mathrm{d}C}{\mathrm{d}t} = k_1 C \tag{1}$$

In this study, k_1 represents the pseudo-first-order rate constant. C represents the concentration of succinonitrile at different oxidation times. When COD is used to indicate the degradation of succinonitrile, this equation can be modified as follows:

$$-\frac{\mathrm{d}C_{(COD)}}{\mathrm{d}t} = k_1 C_{(COD)} \tag{2}$$

This equation, after integration with the boundary conditions $C_{(COD)} = C_{(COD)0}$ for $t = 0$, and $C_{(COD)} = C_{(COD)}$ for $t = t$, leads to:

$$-\ln\left(\frac{C_{(COD)}}{C_{(COD)0}}\right) = -\ln(1-\eta) = k_1 t \tag{3}$$

where η represents the COD removal rate of succinonitrile.

Figure 5(b) shows the pseudo-first-order reaction rate constants of different catalytic ozone systems. The pseudo-first-order reaction rate constants $3.62^{-4}\,\mathrm{min}^{-1}$, $4.34 \times 10^{-3}\,\mathrm{min}^{-1}$ and $7.75 \times 10^{-3}\,\mathrm{min}^{-1}$ correspond to OAS, TCS and MCS respectively. Based on the pseudo-first-order rate constant, the kinetic enhancement of succinonitrile degradation by T2-MOF is more significant than that obtained with other catalysts.

The initial pH of a reaction system is known to be an important factor. Excessive acid/base always seriously affects the efficiency of catalytic reactions and is particularly damaging to heterogeneous catalysts. Therefore, the degradation of succinonitrile by T2-MOF catalyzed ozone at different initial pH values was evaluated. As shown in Figure S6a, T2-MOF was effective over a wide pH range (3.0–7.0). Under excessive acid/base conditions, the COD removal rates were significantly reduced. The likely reasons are as follows. (i) Under excessively acidic conditions, the •OH was rapidly consumed by a large amount of H^+,

which limited the reaction of free radicals with organic matter (Equation (4)). (ii) Under excessively alkaline conditions, the $Fe(OH)_3$ sludge produced by the reaction of the large amount of OH^- with Fe^{3+} could cover the surface of T2-MOF and reduce the efficiency of the catalytic reaction (Equation (5)):

$$\cdot OH + H^+ + e^- \rightarrow H_2O \qquad (4)$$

$$3OH^- + Fe^{3+} \rightarrow Fe(OH)_3 \downarrow \qquad (5)$$

The effect of T2-MOF dosage on succinonitrile decomposition was also investigated. As shown in Figure S5b, with the increase of the dosage of T2-MOF from 10 mg L^{-1} to 40 mg L^{-1}, the COD removal efficiency of succinonitrile increased from 50.6 to 74.3%. This phenomenon might be attributed to the fact that the production of ·OH was accelerated by the great number of active sites that were available with T2-MOF. Nevertheless, succinonitrile decomposition was not enhanced, but slightly decreased (68.3% COD removal efficiency) when the T2-MOF dosage was further increased to 50 mg L^{-1}. The possible reason for this discrepancy was that the agglomeration of T2-MOF limited the diffusion of reactants to the surface of the T2-MOF. Moreover, the excessive T2-MOF added may have consumed ·OH, which reduced the amount of ·OH and hindered the decomposition of succinonitrile (Equation (6)) (Khataee *et al.* 2016):
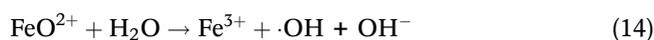
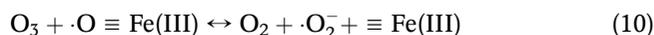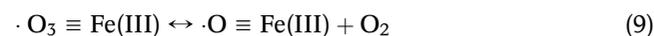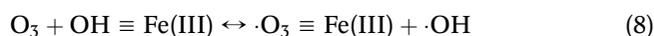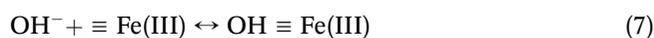$$\cdot OH + \equiv Fe(II) \rightarrow OH^- + \equiv Fe(III) \qquad (6)$$
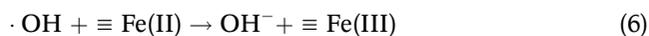
($\equiv$ is the interface of T2-MOF).

In order to understand the mechanism of T2-MOF catalytic ozonation of succinonitrile, water samples from different oxidation times were centrifuged, and the concentrations of Fe^{2+} and total iron ions in the supernatant were determined by o-phenanthroline spectrophotometry. As seen from Figure S6b, in the case where no other iron source was added except T2-MOF, Fe^{2+} and Fe^{3+} were detected in the oxidation system after 30 min. Moreover, the concentrations of Fe^{2+} and Fe^{3+} remained stable from 30 to 150 min. The low concentrations of Fe^{2+} and Fe^{3+} indicated that homogeneous catalysis occurred simultaneously with the heterogeneous catalysis by T2-MOF.

In the heterogeneous catalytic ozonation process, the solid catalyst adsorbs OH^- from the solution onto its surface, which forms a complex with low potential and instability. This complex can react with liquid ozone to produce ·OH (Equations (7)–(9)) (Beltrán *et al.* 2002), which is

the core reaction for heterogeneous catalytic ozonation. The organic matter is rapidly decomposed by ·OH generated according to Equation (8). In the heterogeneous catalytic ozonation, it was difficult for T2-MOF to completely maintain its crystal structure under catalysis, which resulted in some structural damage. A small amount of Fe^{3+} is detached from the solid interface of T2-MOF in a homogeneous catalytic system. In homogeneous catalytic oxidation, chain reactions originate from the Fe^{3+} reaction with water to produce unstable $Fe(OH)^{2+}$ (Equation (11)), which can be decomposed to Fe^{2+} and ·OH when irradiated by weak light (Equation (12)) (Faust & Hoigné 1990). Consequently, homogeneous catalytic oxidation will continue (Equations (13) and (14)) (Løgager *et al.* 1992). The Fe^{3+} consumed in Equation (11) is replenished according to Equation (14). Therefore, the circulation of Fe^{3+} and Fe^{2+} in the liquid phase is the key to maintaining continuous homogeneous catalytic ozonation:

$$OH^- + \equiv Fe(III) \leftrightarrow OH \equiv Fe(III) \qquad (7)$$

$$O_3 + OH \equiv Fe(III) \leftrightarrow \cdot O_3 \equiv Fe(III) + \cdot OH \qquad (8)$$

$$\cdot O_3 \equiv Fe(III) \leftrightarrow \cdot O \equiv Fe(III) + O_2 \qquad (9)$$

$$O_3 + \cdot O \equiv Fe(III) \leftrightarrow O_2 + \cdot O_2^- + \equiv Fe(III) \qquad (10)$$

$$Fe^{3+} + H_2O \rightarrow Fe(OH)^{2+} + H^+ \qquad (11)$$

$$Fe(OH)^{2+} + h\upsilon \rightarrow Fe^{2+} + \cdot OH \qquad (12)$$

$$Fe^{2+} + O_3 \rightarrow FeO^{2+} + O_2 \qquad (13)$$

$$FeO^{2+} + H_2O \rightarrow Fe^{3+} + \cdot OH + OH^- \qquad (14)$$

If the structure of the T2-MOF is unstable, Fe^{3+} will continuously detach from the interface of T2-MOF and enter the liquid phase. From the perspective of chemical reaction kinetics, the concentration of Fe^{2+} will increase with Fe^{3+} (Equations (11) and (12)). At the same time, the reaction of Equations (11) and (14) will be accelerated. However, as shown in Figure S6b, the concentrations of Fe^{2+} and Fe^{3+} in the ozonation system did not obviously increase after 30 min. In addition, the sum of the concentrations of Fe^{2+} and Fe^{3+} was much smaller than the concentration of T2-MOF. This result indicated that the structure of T2-MOF was stable, in contrast to expectations. The most important conclusion is that T2-MOF is an efficient catalyst for catalyzing ozone to degrade succinonitrile. The mechanism for the ozonation of succinonitrile catalyzed by T2-MOF is shown in Figure 6.
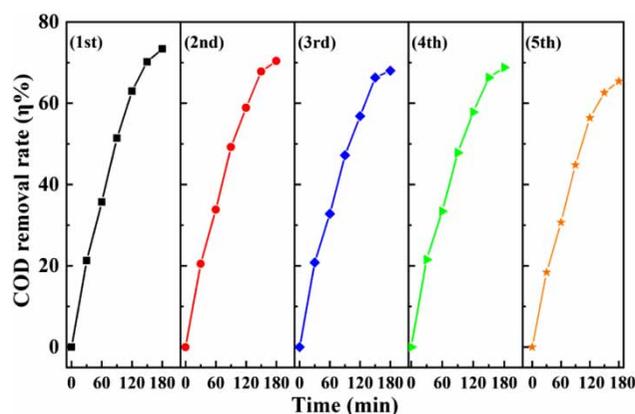
Figure 6 | Mechanism for the ozonation of succinonitrile catalyzed by T2-MOF.

Effect of inorganic anions on catalytic ozonation

Figure 7 shows the results of catalytic performance under three inorganic salts (Na_2SO_4, NaCl and Na_2CO_3) and the corresponding degradation efficiency sequence was: $Na_2SO_4 > Na_2CO_3 > NaCl$. The result indicated that Na_2SO_4 had a slight effect on the ozonation of succinonitrile, because in neutral solution, Na_2SO_4 could not change the reaction environment. But in reactive systems with added NaCl and Na_2CO_3, the degradation efficiency of succinonitrile clearly reduced by 42.1% and 33.1%. This result might be ascribed to the fact that both chloride and carbonate could consume free radicals quickly, because they have higher reaction rate constants with several free radicals commonly found in AOPs (Equations (1)–(7)) (Yang *et al.* 2014):

$$\cdot OH + CO_3^{2-} \rightarrow CO_3^{-} + OH^{-} \quad k = 3.9 \times 10^8 \, M^{-1}s^{-1} \quad (15)$$

$$\cdot OH + HCO_3^{-} \rightarrow CO_3^{-} + H_2O \quad k = 8.6 \times 10^6 \, M^{-1}s^{-1} \quad (16)$$

$$O_2^{-} + CO_3^{-} \rightarrow CO_3^{2-} + O_2 \quad k = 6 \times 10^8 \, M^{-1}s^{-1} \quad (17)$$

$$\cdot OH + Cl^{-} \rightarrow ClOH^{\cdot -} \quad k = 4.3 \times 10^9 \, M^{-1}s^{-1} \quad (18)$$

$$ClOH^{\cdot -} + H^{+} \rightarrow Cl \cdot + H_2O \quad k = 2.1 \times 10^{10} \, M^{-1}s^{-1} \quad (19)$$

$$Cl^{-} + Cl\cdot \rightarrow Cl_2^{-} \quad k = 8.5 \times 10^9 \, M^{-1}s^{-1} \quad (20)$$

$$Cl_2^{-} + O_2^{-} \rightarrow 2Cl^{-} + O_2 \quad k = 2 \times 10^9 \, M^{-1}s^{-1} \quad (21)$$

Reusability test of T2-MOF

Five successive cycles of degradation testing were carried out to evaluate the reusability of T2-MOF. As shown in Figure 8, the COD removal efficiency of succinonitrile decreases slightly in every run, but is still as high as 65.4% after the fifth cycle. Compared with the first cycle, the COD removal rate had only decreased by 8%, which indicated that T2-MOF had reusability.

Figure 7 | Effect of different inorganic anions on catalytic ozonation.

Figure 8 | Reusability and stability of T2-MOF in catalytic ozonation.

CONCLUSION

In summary, T2-MOF was synthesized as a catalyst based on $FeCl_3.6H_2O$ and $C_4H_6O_6$, and had a uniform three-dimensional structure. The T2-MOF showed excellent catalytic efficiency for catalytic ozonation of succinonitrile. The catalytic activities were closely dependent on the various operating parameters, such as initial pH, HRT, and T2-MOF dosage. Under optimal conditions, the average COD removal rate of succinonitrile reached 73.1% within 180 min. This result was 12.6 times COD removal rate compared to using ozone alone. In addition, stable catalytic activity was maintained over a wide pH range (3.0–7.0). Moreover, stable concentrations of Fe^{2+} and Fe^{3+} were detected in the liquid phase of the reaction system, indicating that heterogeneous catalyzed ozonation and homogeneous catalytic ozonation occurred simultaneously in the reaction system, which was very beneficial for the degradation of succinonitrile. This study provides a new inexpensive material for wastewater treatment containing refractory organic pollutants.

ACKNOWLEDGEMENTS

COMPLIANCE WITH ETHICAL STANDARDS

The authors declare that they have no competing interests.

DATA AVAILABILITY STATEMENT

All relevant data are included in the paper or its Supplementary Information.

REFERENCES

Ahimou, F., Boonaert, C. J. P., Adriaensen, Y., Jacques, P., Thonart, P., Paquot, M. & Rouxhet, P. G. 2007 XPS analysis of chemical functions at the surface of *Bacillus subtilis*. *Journal of Colloid and Interface Science* **309** (1), 49–55.

An, P., Xu, X. C., Yang, F. L., Zhang, H. M. & Wang, M. M. 2011 Treatment of acrylic fiber wastewater by synergistic effect of O_3/UV. *Journal of Civil, Architectural & Environmental Engineering* **33** (1), 135–139.

Araya, T., Jia, M., Yang, J., Zhao, P., Cai, K., Ma, W. & Huang, Y. 2017 Resin modified MIL-53 (Fe) MOF for improvement of photocatalytic performance. *Applied Catalysis B: Environmental* **203**, 768–777.

Baldanza, S., Ardini, J., Giglia, A. & Held, G. 2016 Stereochemistry and thermal stability of tartaric acid on the intrinsically chiral Cu{531} surface. *Surface Science* **643**, 108–116.

Beltrán, F. J., Rivas, J., Álvarez, P. & Montero-de-Espinosa, R. 2002 Kinetics of heterogeneous catalytic ozone decomposition in water on an activated carbon. *Ozone: Science & Engineering* **24** (4), 227–237.

Benitez, F. J., Beltran-Heredia, J., Acero, J. L. & Rubio, F. J. 1999 Chemical decomposition of 2,4,6-trichlorophenol by ozone, Fenton's reagent, and UV radiation. *Industrial & Engineering Chemistry Research* **38** (4), 1341–1349.

Chandra, V., Park, J., Chun, Y., Lee, J. W., Hwang, I. C. & Kim, K. S. 2010 Water-dispersible magnetite-reduced graphene oxide composites for arsenic removal. *ACS Nano* **4** (7), 3979–3986.

Chong, M., Jin, B., Chow, C. W. K. & Saint, C. 2010 Recent developments in photocatalytic water treatment technology: a review. *Water Research* **44** (10), 2997–3027.

Easun, T. L., Moreau, F., Yan, Y., Yang, S. & Schröder, M. 2017 Structural and dynamic studies of substrate binding in porous metal–organic frameworks. *Chemical Society Reviews* **46**, 239–274.

Faust, B. C. & Hoigné, J. 1990 Photolysis of Fe (III)-hydroxy complexes as sources of OH radicals in clouds, fog and rain. *Atmospheric Environment. Part A. General Topics* **24** (4), 79–89.

Gassie, L. W. & Englehardt, J. D. 2017 Advanced oxidation and disinfection processes for onsite net-zero greywater reuse: a review. *Water Research* **125**, 384–399.

Gayen, P., Chen, C., Abiade, J. T. & Chaplin, B. P. 2018 Electrochemical oxidation of atrazine and clothianidin on Bi-doped SnO_2–Ti_nO_{2n-1} electrocatalytic reactive electrochemical membranes. *Environmental Science & Technology* **52** (21), 12675–12684.

Guo, P., Dutta, D., Wong-Foy, A. G., Gidley, D. W. & Matzger, A. J. 2015 Water sensitivity in Zn_4O-based MOFs is structure

and history dependent. *Journal of the American Chemical Society* **137** (7), 2651–2657.

Hermes, S., Schröder, F., Amirjalayer, S., Schmid, R. & Fischer, R. A. 2006 Loading of porous metal–organic open frameworks with organometallic CVD precursors: inclusion compounds of the type [LnM]a@MOF-5. *Journal of Materials Chemistry* **16** (25), 2464–2472.

Hidalgo, A. M., Gómez, M., Murcia, M. D., Serrano, M., Rodríguez-Schmidt, R. & Escudero, P. A. 2018 Behaviour of polysulfone ultrafiltration membrane for dyes removal. *Water Science & Technology* **77** (8), 2093–2100.

Hu, N., Wu, Z., Ding, L., Li, R., Huang, D., Li, H. & Zheng, H. 2016 Removal of polyacrylonitrile oligomers from acrylic fiber wastewater using two-stage flotation. *Chemical Engineering Journal* **306**, 186–192.

Huang, X. P., Hou, X. J., Zhao, J. C. & Zhang, L. Z. 2016 Hematite facet confined ferrous ions as high efficient Fenton catalysts to degrade organic contaminants by lowering H_2O_2 decomposition energetic span. *Applied Catalysis B: Environmental* **181**, 127–137.

Khataee, A., Gholami, P., Sheydaei, M., Khorram, S. & Joo, S. W. 2016 Preparation of nanostructured pyrite with N_2 glow discharge plasma and the study of its catalytic performance in the heterogeneous Fenton process. *New Journal of Chemistry* **40** (6), 5221–5230.

Kim, J., Chen, B., Reineke, T. M., Li, H., Eddaoudi, M., Moler, D. B., O'Keeffe, M. & Yaghi, O. M. 2001 Assembly of metal – organic frameworks from large organic and inorganic secondary building units: new examples and simplifying principles for complex structures. *Journal of the American Chemical Society* **123** (34), 8239–8247.

Li, Y. J., Shang, X. L., Li, C. H., Huang, X. M. & Zheng, J. J. 2018 Novel p–n junction UiO-66/BiOI photocatalysts with efficient visible-light-induced photocatalytic activity. *Water Science & Technology* **77** (5), 1441–1448.

Lian, L., Yao, B., Hou, S., Fang, J., Yan, S. & Song, W. 2017 Kinetic study of hydroxyl and sulfate radical-mediated oxidation of pharmaceuticals in wastewater effluents. *Environmental Science & Technology* **51** (5), 2954–2962.

Løgager, T., Holcman, J., Sehested, K. & Pedersen, T. 1992 Oxidation of ferrous ions by ozone in acidic solutions. *Inorganic Chemistry* **31** (17), 3523–3529.

Mohapatra, D. P. & Kirpalani, D. M. 2019 Selenium in wastewater: fast analysis method development and advanced oxidation treatment applications. *Water Science & Technology* **79** (5), 842–849.

Peng, L., Zhang, J., Li, J., Han, B., Xue, Z. & Yang, G. 2012 Surfactant-directed assembly of mesoporous metal–organic framework nanoplates in ionic liquids. *Chemical Communications* **48** (69), 8688–8690.

Sun, M., Chen, F., Qu, J., Liu, H. & Liu, R. 2015 Optimization and control of Electro-Fenton process by pH inflection points: a case of treating acrylic fiber manufacturing wastewater. *Chemical Engineering Journal* **269**, 399–407.

Tang, J. & Wang, J. 2018 Metal organic framework with coordinatively unsaturated sites as efficient Fenton-like catalyst for enhanced degradation of sulfamethazine. *Environmental Science & Technology* **52** (9), 5367–5377.

Wei, J., Song, Y., Tu, X., Zhao, L. & Zhi, E. 2013 Pretreatment of dry-spun acrylic fiber manufacturing wastewater by Fenton process: optimization, kinetics and mechanisms. *Chemical Engineering Journal* **218**, 319–326.

Yaghi, O. M., Li, G. & Li, H. 1995 Selective binding and removal of guests in a microporous metal–organic framework. *Nature* **378**, 703–706.

Yaghi, O. M., O'Keeffe, M., Ockwig, N. W., Chae, H. K., Eddaoudi, M. & Kim, J. 2003 Reticular synthesis and the design of new materials. *Nature* **423**, 705–714.

Yang, Y., Pignatello, J. J., Ma, J. & Mitch, W. A. 2014 Comparison of halide impacts on the efficiency of contaminant degradation by sulfate and hydroxyl radical-based advanced oxidation processes (AOPs). *Environmental Science & Technology* **48** (4), 2344–2351.

Yu, D., Wu, M., Hu, Q., Wang, L., Lv, C. & Zhang, L. 2019 Iron-based metal-organic frameworks as novel platforms for catalytic ozonation of organic pollutant: efficiency and mechanism. *Journal of Hazardous Materials* **367**, 456–464.

Zeng, T., Zhang, X., Wang, S., Niu, H. & Cai, Y. 2015 Spatial confinement of a Co_3O_4 catalyst in hollow metal–organic frameworks as a nanoreactor for improved degradation of organic pollutants. *Environmental Science & Technology* **49** (4), 2350–2357.

Zhang, C. H., Ai, L. H. & Jiang, J. 2015 Solvothermal synthesis of MIL–53(Fe) hybrid magnetic composites for photoelectrochemical water oxidation and organic pollutant photodegradation under visible light. *Journal of Materials Chemistry A* **3** (6), 3074–3081.

Zhong, L. B. 2017 *Study on Catalytic Ozonation of Typical Pollutants in Acrylic Fibers Wastewater by Metal Chelates.* Northeast Petroleum University, Daqing City.

Zhou, H. C., Long, J. R. & Yaghi, O. M. 2012 Introduction to metal-organic frameworks. *Chemical Reviews* **112** (2), 673–674.